Bangladesh J. Bot. **54**(4): 1005-1013, 2025 (December) DOI: https://doi.org/10.3329/bjb.v54i4.86576

INVESTIGATION OF *EPHEDRA ALTISSIMA* COMPOUNDS: HISTOLOGICAL INSIGHTS AND IN SILICO TARGETING OF DIHYDROFOLATE REDUCTASE IN *ASPERGILLUS FLAVUS*

HOUAS YAMINA*, HASSANI FAICAL, ABDELLI IMANE[1,2], GHALEM SARRA AND BEKKAL BEREKSI SOHAYB

Laboratory of Ecology and Management of Natural Ecosystems, Faculty Snv-Stu, University of Tlemcen, Algeria

Keywords: Ephedra altissima, Histological study, *In silico* study, *Aspergillus flavus,* Aflatoxins

Abstract

Ephedra is a medicinal plant well known for its therapeutic properties, primarily attributed to its bioactive compounds. Recent studies have highlighted its antifungal potential, particularly against *Aspergillus flavus*, a phytopathogenic fungus responsible for aflatoxin production. However, studies on this topic remain limited. The present study aimed to investigate the anatomical adaptations of *Ephedra altissima* stems and to evaluate the antifungal activity of its flavonoid compounds. A detailed histological analysis was performed, complemented by an in silico study, which confirmed the strong antifungal activity of these compounds. These findings highlight the potential of *Ephedra* as a natural agent for managing fungal pathogens in both agriculture and healthcare.

Introduction

Ephedra altissima, a medicinal plant native to North Africa and parts of Southern Europe, is recognized for its traditional therapeutic uses and bioactive compounds, including ephedrine and pseudoephedrine (Edrah *et al.* 2016). These alkaloids are widely used in treating respiratory disorders and as stimulants in dietary supplements. The species grows in arid and semi-arid environments, where it faces water scarcity and high temperatures, which may have driven specific anatomical and physiological adaptations (Ickert-Bond and Renner 2016).

Despite its pharmacological importance, research on *E. altissima* remains limited. Few studies have investigated its anatomical features, which are crucial for understanding how the plant survives under extreme environmental conditions, or its potential as a source of natural antifungal agents. In particular, *Aspergillus flavus*, a major producer of aflatoxins, poses a serious threat to staple crops and human health, highlighting the need for eco-friendly antifungal strategies (Abdelaziz *et al.* 2022).

The present study addresses this gap through a combined histological and in silico approach. The anatomical analysis focuses on vascular and protective tissues to reveal adaptations to arid conditions, while the in silico study evaluates the antifungal potential of flavonoid compounds from *E. altissima*. This interdisciplinary approach aims to enhance both botanical understanding and the development of natural antifungal agents with potential applications in agriculture and healthcare. Our previous experience in histology (Ghalem and Hassani 2019), provided the methodological basis for accurate and reproducible anatomical and histometric analyses, which were applied in the present study to investigate the structural features of *E. altissima*.

*Author for correspondence: <yaminahouas6@gmail.com>. [1]Ecole Supérieure en Sciences Appliquées, ESSA-Tlemcen, BP 165 RP Bel Horizon, Tlemcen 13000, Algeria. [2]Laboratory of Natural and Bio-actives Substances, Faculty of Science, University of Tlemcen, Algeria.

Materials and Methods

This study integrated anatomical and computational approaches to evaluate the biological potential of *Ephedra altissima*.

Stem samples of *E. altissima* were collected from the Tlemcen region (Algeria) between May and June 2023 and identified at the University of Tlemcen. To investigate the plant's anatomical adaptations, both young and mature stems were examined. Manual crosssections were prepared, stained with methylene blue and carmine alum to differentiate vascular tissues, and observed under a light microscope equipped with a digital camera.

Histometric measurements were conducted manually using a histometer, allowing precise quantification of vascular tissues and other anatomical structures.

To evaluate the antifungal potential of bioactive compounds from *E. altissima*, molecular docking was performed using ephedrine, norephedrine, quercetin, and kaempferol as ligands.

The target protein, *Aspergillus flavus* dihydrofolate reductase (DHFR, PDB ID: 6DRS, resolution 2.00 Å), was prepared using Discovery Studio 2020 and AutoDock Tools. Ligand structures were retrieved from PubChem and converted using Open Babel. Docking simulations were performed with AutoDock Vina v0.8 to calculate binding affinities, and Discovery Studio Biovia was used to analyze protein-ligand interactions.

Fig. 1. (A) Branches of *Ephedra altissima* mature berry-like fruits and overall reproductive morphology. (B) Close-up of vegetative twigs displaying the photosynthetic cladodes and young developing buds.

Results and Discussion

Despite numerous studies on various *Ephedra* species, data on *E. altissima* remain limited, particularly regarding its histology. Previous investigations by Thompson (1912), Gifford (1943), and Dörken (2012) have only briefly addressed its anatomical features. The present study aimed to reveal the structure of vegetative organs of *E. altissima*, with findings illustrated in Figs 2-6.

Ephedra altissima produces two juvenile shoot types: a dominant primary shoot and a smaller, short-lived secondary shoot, both sharing similar anatomical characteristics (Gifford 1943). The epidermis consists of quadrangular cells with thick walls and a thick cuticle, featuring numerous sunken stomata within vertical ridges. Beneath these ridges, clusters of non-lignified fibers overlay a spongy parenchyma layer. The cortex contains isolated or grouped lignified fibers, while the pericycle has lignified fiber bundles adjacent to the phloem. The vascular system

comprises 14-15 radially arranged xylem and phloem bundles surrounding a broad parenchymatous central pith, some cells containing brown pigments. In larger stems, a central hollow pith enhances flexibility and climbing ability (Mezogi *et al*. 2020).

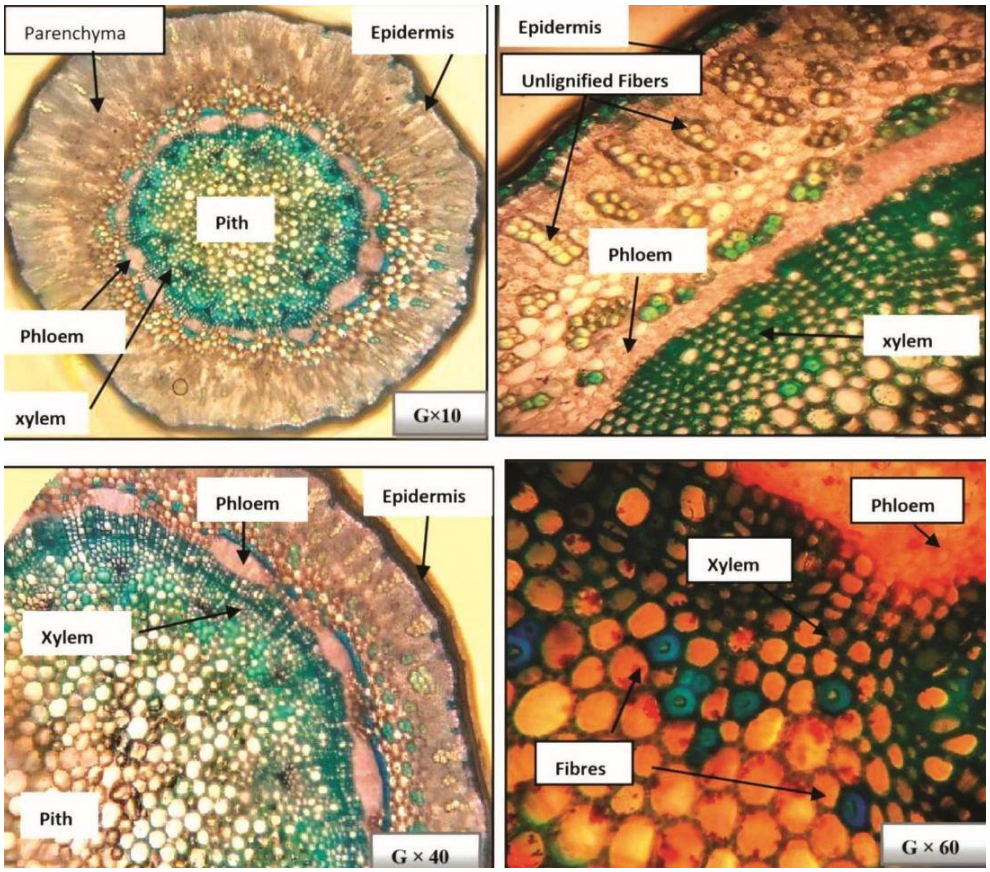

Fig. 2. Transverse sections of young stems of *Ephedra altissima* showing the organization of primary tissues, including epidermis, parenchyma, phloem, xylem, pith, and lignified fibers at different magnifications (G×10, G×40, G×60).

Stomata in *E. altissima* are tetracytic, composed of four epidermal cells including two guard cells surrounding the pore (Barrera 2013). In mature stems, the epidermis is single layered and highly cutinized, providing protection over the underlying parenchyma. Vascular bundles are reinforced with lignified fibers, and xylem vessels are prominent, whereas resin ducts are absent. Histometric analysis (Table 1 and Fig. 7) demonstrates that the anatomical structure of *E. altissima* undergoes notable modifications as stems mature. A pronounced increase in xylem thickness (2.3 to 6.7 µm) reflects strengthened mechanical support and enhanced hydraulic efficiency, while the pith expands slightly. Conversely, the marked reduction in parenchyma and non-lignified fibers indicates a developmental shift toward greater tissue specialization for support and conduction. The epidermis and phloem exhibit only minor changes, pointing to a relatively stable functional role. Collectively, these trends underscore the adaptation of mature stems toward a more rigid and efficient anatomical configuration typical of xerophytic species.

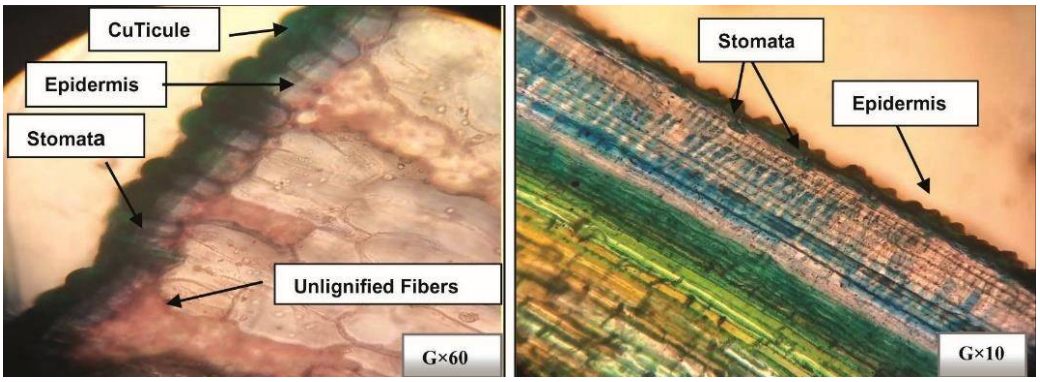

Fig. 3. Longitudinal sections of the stem epidermis of *Ephedra altissima* showing the cuticle, epidermal cells, stomata, and unlignified fibers at different magnifications. (G×10, G×60).

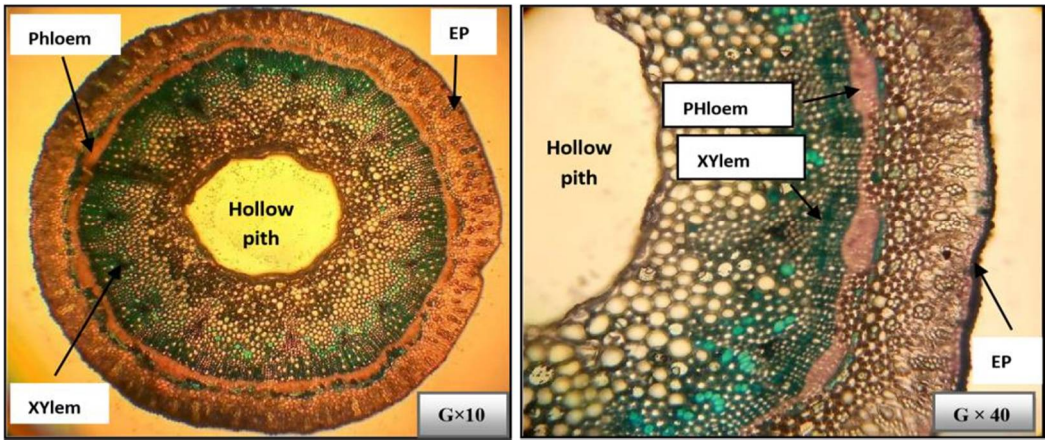

Fig. 4. Cross section of a large young stem showing the hollow pith and the concentric arrangement of vascular tissues, with well-defined xylem and phloem rings beneath the epidermis (EP) at different magnifications. (G×10, G×40).

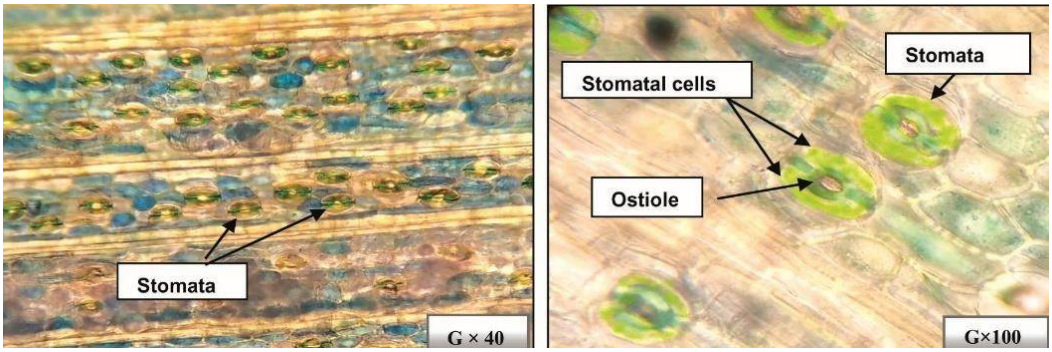

Fig. 5. Epidermal surface structure of *Ephedra altissima*, showing longitudinal rows of stomata and detailed views of the stomatal complex including stomatal cells, ostiole, and surrounding epidermal cells.

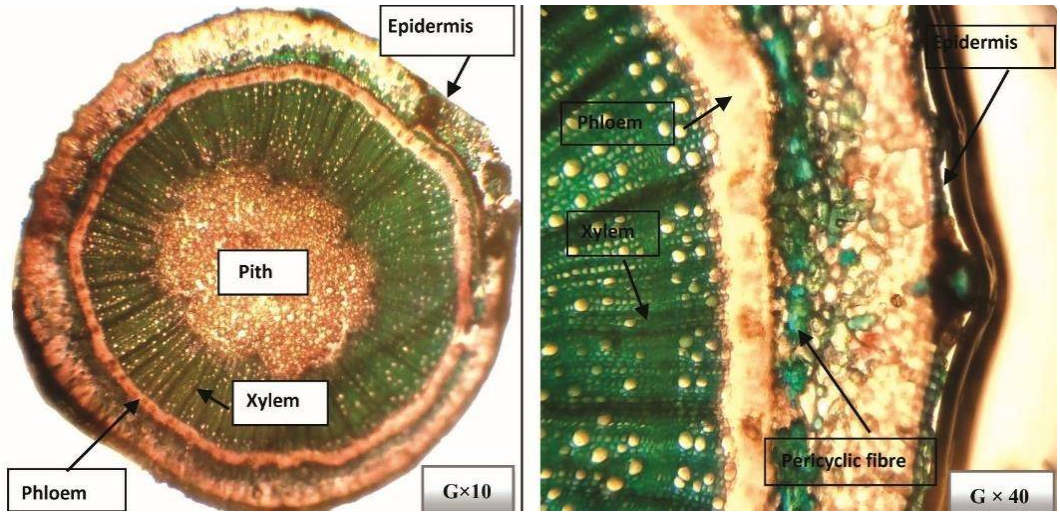

Fig. 6. Transverse sections of an old stem of *Ephedra altissima*, showing the central pith, well developed xylem and phloem tissues, the epidermis, and the ring of pericyclic fibres characteristic of mature stems.

Table 1. Comparative average histometric measurements of young and mature stems of *Ephedra altissima*.

Tissus / Mean of measurements (µm)	Epidermis	Non-lignified fibers	Parenchyma	Pericyclic fibers	Phloem	Xylem	Pith
Young stems	1,2	3,4	6	2,4	1,4	2,3	4,5
Mature stems	1.4	1.6	2	1.6	1.6	6.7	5.2

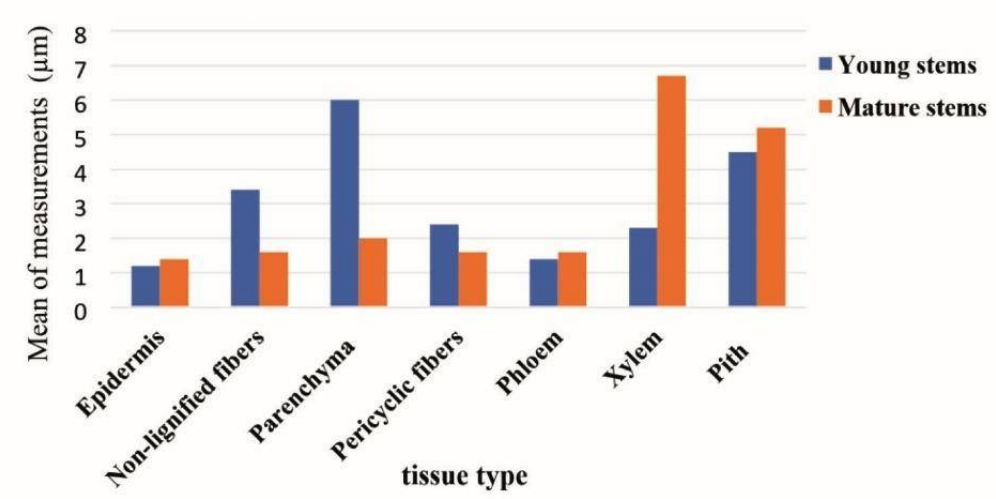

Fig. 7. Comparative bar chart illustrating the average histometric measurements of different tissue types in young and mature stems of *Ephedra altissima*. The X-axis represents the anatomical categories (epidermis, non-lignified fibres, parenchyma, pericyclic fibres, phloem, xylem and pith). The Y-axis indicates the mean histometric values expressed in micrometres (µm).

Table 2. Docking scores between protein dihydrofolate reductase from *A. flavus* and the compounds extracted from *E. alsinoea*.

		Dihydrofolate reductase (PDB ID:6OR8)								
ligands	S-score (kcal/mol)	Names	Color	Distance (Å)	Category	Types	From	From chemestry	To	To chemestry
Kaempferol	-8.3	A:THR66:HG1 - :UNL1:O		2.40822	Hydrogen Bond	Conventional Hydrogen Bond	A:THR66:HG1	H-Donor	:UNL1:O	H- Acceptor
		:UNL1:H - :UNL1:O		1.7918	Hydrogen Bond	Conventional Hydrogen Bond	:UNL1:H	H-Donor	:UNL1:O	H- Acceptor
		A:GLY27:CA - :UNL1:O		3.34061	Hydrogen Bond	Carbon Hydrogen Bond	A:GLY27:CA	H-Donor	:UNL1:O	H- Acceptor
		A:GLY27:CA - :UNL1:O		3.24618	Hydrogen Bond	Carbon Hydrogen Bond	A:GLY27:CA	H-Donor	:UNL1:O	H- Acceptor
		A:GLY158:CA - :UNL1:O		3.22527	Hydrogen Bond	Carbon Hydrogen Bond	A:GLY158:CA	H-Donor	:UNL1:O	H- Acceptor
		A:THR197:CG2 - :UNL1		3.98528	Hydrophobic	Pi-Sigma	A:THR197:CG2	C-H	:UNL1	H- Acceptor
		:UNL1 - A:LYS65		4.65292	Hydrophobic	Pi-Alkyl	:UNL1	Pi-Orbitals	A:LYS65	Pi-Orbitals
		:UNL1 - A:ILE26		5.42516	Hydrophobic	Pi-Alkyl	:UNL1	Pi-Orbitals	A:ILE26	Alkyl
Epinephrine	-6.5	A:ALA12:HN - :UNL1:O		2.34285	Hydrogen Bond	Conventional Hydrogen Bond	A:ALA12:HN	H-Donor	:UNL1:O	H- Acceptor
		:UNL1:H - A:ILE156:O		2.03852	Hydrogen Bond	Conventional Hydrogen Bond	:UNL1:H	H-Donor	A:ILE156:O	H- Acceptor
		:UNL1:H -A:TYR162:OH		2.47115	Hydrogen Bond	Conventional Hydrogen Bond	:UNL1:H	H-Donor	A:TYR162:OH	H- Acceptor
		A:PHE44 - :UNL1		3.89499	Hydrophobic	Pi-Pi Stacked	A:PHE44	Pi-Orbitals	:UNL1	Pi-Orbitals
		:UNL1 - A:ILE156		5.48383	Hydrophobic	Pi-Alkyl	:UNL1	Pi-Orbitals	A:ILE156	Pi-Orbitals
Norepinephrine	-6.1	:UNL1:H - A:ILE156:O		2.9267	Hydrogen Bond	Conventional Hydrogen Bond	:UNL1:H	H-Donor	A:ILE156:O	H- Acceptor
		:UNL1:H - A:TYR162:OH		2.15579	Hydrogen Bond	Conventional Hydrogen Bond	:UNL1:H	H-Donor	A:TYR162:OH	H- Acceptor
		A:MET41:SD - :UNL1		5.70099	Other	Pi-Sulfur	A:MET41:SD	Sulfur	:UNL1	Pi-Orbitals
		A:PHE44 - :UNL1		3.71623	Hydrophobic	Pi-Pi Stacked	A:PHE44	Pi-Orbitals	:UNL1	Pi-Orbitals

Table. 3 Docking scores between the protein from *protein dihydrofolate reductase from A. flavus and* ligands of fungicides.

		dihydrofolate reductase (PDB ID:6DRS)								
ligands	S-score (kcal/mol)	Names	Color	Distance ( )	Category	Types	From	From chemestry	To	To chemestry
voriconazol	-6.0	A:THR66:HN - :UNL1:O		2,25174	Hydrogen Bond	Conventional Hydrogen Bond	A:THR66:HN	H-Donor	:UNL1:O	H- Acceptor
		A:GLY158:HN - :UNL1:O		2,20911	Hydrogen Bond	Conventional Hydrogen Bond	A:GLY158:HN	H-Donor	:UNL1:O	H- Acceptor
		A:ALA159:HN - :UNL1:N		2,72413	Hydrogen Bond	Conventional Hydrogen Bond	A:ALA159:HN	H-Donor	:UNL1:O	H- Acceptor
		A:GLY158:CA - :UNL1		3,93579	Hydrophobic	Pi-Sigma	A:GLY158:CA	C-H	:UNL1	Pi-Orbitals
		A:ALA12:HN - :UNL1:N		1,9845	Hydrogen Bond	Conventional Hydrogen Bond	A:ALA12:HN	H-Donor	:UNL1:N	H- Acceptor
		:UNL1:H - :UNL1:N		1,92815	Hydrogen Bond	Conventional Hydrogen Bond	:UNL1:H	H-Donor	:UNL1:N	H- Acceptor
		:UNL1:C - A:ILE10:O		3,63829	Hydrogen Bond	Carbon Hydrogen Bond	:UNL1:C	H-Donor	A:ILE10:O	H- Acceptor
		:UNL1:C - A:ILE10:O		3,04601	Halogen	Halogen (Fluorine)	A:ILE156:O	Halogen Acceptor	:UNL1:F	Halogen
		A:ILE156:O - :UNL1:F		3,73791	Hydrophobic	Halogen (Fluorine)	A:LEU32:CD2	C-H	:UNL1	Pi-Orbitals
		A:THR66:CG2 - :UNL1		3,78324	Hydrophobic	Pi-Sigma	A:THR66:CG2	C-H	:UNL1	Pi-Orbitals
		:UNL1:C - A:PHE44		3,78318	Hydrophobic	Pi-Sigma	:UNL1:C	C-H	A:PHE44	Pi-Orbitals
carbendazim	-6.8	:UNL1 - A:ALA12		4,77813	Hydrophobic	Pi-Sigma	:UNL1	Pi-Orbitals	A:ALA12	Alkyl
		:UNL1 - A:VAL70		4,43191	Hydrophobic	Pi-Alkyl	:UNL1	Pi-Orbitals	A:VAL70	Alkyl
		:UNL1 - A:LEU77		5,46409	Hydrophobic	Pi-Alkyl	:UNL1	Pi-Orbitals	A:LEU77	----Alkyl

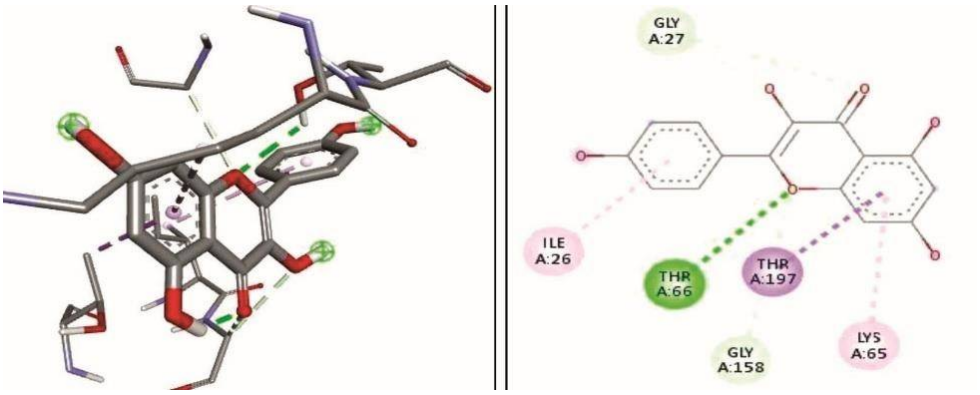

Fig. 8. Illustration of the binding conformation of Kaempferol within the active site of dihydrofolate reductase, alongside the 2D interaction map highlighting the key amino acid residues involved in ligand stabilization.

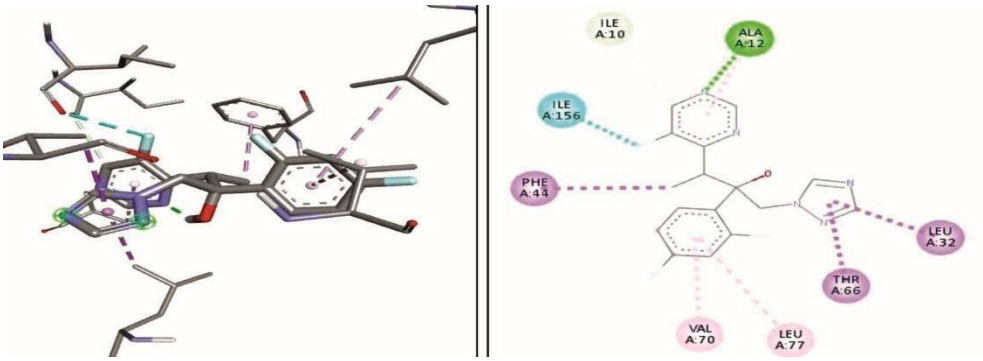

Fig. 9. Illustration of the binding conformation of carbendazim within the active site of dihydrofolate reductase, alongside the 2D interaction map highlighting the key amino-acid residues involved in ligand stabilization.

Molecular docking simulations (Table 2 and 3) evaluated interactions between bioactive compounds from *E. altissima* (ephedrine, norephedrine, and kaempferol) and *A. flavus* dihydrofolate reductase (DHFR, PDB ID: 6DRS). Kaempferol showed the strongest binding affinity (-8.3 kcal/mol), forming multiple hydrogen bonds with residues THR66, GLY27, and GLY158, along with hydrophobic and π-interactions. Ephedrine and norephedrine displayed moderate affinities (6.5 and -6.1 kcal/mol), whereas reference antifungal agents carbendazim (-6.8 kcal/mol) and voriconazole (-6.0 kcal/mol) exhibited lower binding strengths than kaempferol. These results indicate that kaempferol is a promising natural DHFR inhibitor, potentially hindering fungal growth and reducing aflatoxin production.

The histological observations, including a thick cuticle, compact mesophyll with reduced 1*altissima*'s adaptations to arid environments, promoting water conservation and mechanical resistance. Combined with in silico findings, this study demonstrates the plant's potential as a source of natural antifungal compounds, offering eco-friendly alternatives to synthetic fungicides with reduced toxicity and lower risk of resistance.

Overall, the integrated anatomical and molecular investigation underscores the importance of *E. altissima* as both a medicinal plant and a promising source of bioactive molecules for sustainable fungal disease management in agriculture and healthcare.

Acknowledgments

We sincerely thank the University of Tlemcen for its logistical and technical support, as well as our Department for assistance in plant identification and the acquisition of microscopic data. We also appreciate our colleagues for their encouragement and constructive suggestions.

References

Abdelaziz AM, El-Wakil DA, Attia MS, Ali OM, AbdElgawad H and Hashem AH 2022. Inhibition of *Aspergillus flavus* growth and aflatoxin production in *Zea mays* L. using endophytic *Aspergillus fumigatus*. J. Fungi (Basel) **8**(5): 482.

Barrera SM JA, Pozner R and Di Stilio VS 2013. Leaf morphology and anatomy in *Ephedra altissima* Desf. (Ephedraceae, Gnetales) and their evolutionary relevance. Feddes Rep. **123**(1-2): 33-41.

Dörken VM 2012. Leaf morphology and anatomy in *Ephedra altissima* Desf. (Ephedraceae, Gnetales) and their evolutionary relevance. Feddes Rep. **123**(1-2): 33-41.

Edrah SM, Aljenkawi A, Omeman A and Alafid F 2016. Qualitative and quantitative analysis of phytochemicals of various extracts from *Ephedra altissima* from Libya. J. Med. Plants Stud. **4**: 119121.

Ghalem S and Hassani F 2019. Histological study of *Lavatera maritima* in the region of Marsa Ben M'hidi (Tlemcen, Algeria). Am. J. Sci. Eng. Technol. **4**(2): 30-33.

Gifford EM Jr 1943.The structure and development of the shoot apex of *Ephedra altissima* Desf. *Bull.* Torrey Bot. Club **70**(1): 15-25.

Ickert-Bond SM and Renner SS 2016. The Gnetales: Recent insights on their morphology, reproductive biology, chromosome numbers, biogeography, and divergence times. J. Syst. Evol. **54**(1): 1-16.

Mezogi J, Abusaida H, El H, Shibani N, Dali A, Abuelkhair K, Shalabi S and Aburawi S 2020. Effect of subtoxic dose of *Ephedra altissima* methanolic extract on reproductive system of male albino mice. J. Med. Plants Stud. **8**(3): 45-52.

Thompson W.P. 1912. The anatomy and relationships of Gnetales. I. The genus *Ephedra*. *Ann. Bot.* **26**(104): 1077–1104

(Manuscript received on 10 July, 2025; revised on 29 November, 2025)